DEM modeling of ice cuttings transportation by electromechanical auger core drills

J. HONG, P. TALALAY, M. SYSOEV, X. FAN

Polar Research Center, Jilin University, Changchun, China
E-mail: ptalalay@yahoo.com

ABSTRACT. Electromechanical auger core drills are widely used in shallow ice-coring practice on mountain glaciers and polar ice caps and sheets. Generally, these drills are lightweight, can be readily transported to remote drilling sites, are easily installed there and drill with relatively high rates of penetration and low power consumption. During the past few decades, dozens of electromechanical auger drills have been designed. However, the auger options were usually determined by experience, and the main parameters (auger angle and rotation speed) are varied in a wide range from drill to drill. In order to choose the optimal auger parameters, the discrete element method (DEM) is used to analyze the performance of cuttings transportation for different rotation speeds in the range 50–200 rpm and auger angles in the range 15–45°. To improve the efficiency of cuttings transportation, many factors have to be considered (e.g. particle sizes and their variability, ice temperature, material of the core barrel and jacket, and availability of needed driven motor-gears). For the conditions assumed in the present studies, the recommended rotation speed is 100 rpm at auger angles of 35–40°.

KEYWORDS: ice coring

INTRODUCTION

Shallow drilling in ice sheets and glaciers down to 300–350 m depth has valuable applications for glacier structure, composition and thermodynamics study and for research into current climate variability (e.g. inter-hemispheric relationships and the timing and expression of the Little Ice Age). These tasks were included in the project '2k Array' for the next decade or more of the ice-core community under the auspices of International Partnerships in Ice Core Sciences (IPICS; http://www.pages-igbp.org/ipics/). Electromechanical auger core drills are widely used in ice shallow-coring practice given their obvious advantages: (1) they are lightweight and can be readily transported by helicopter; (2) power consumption is relatively low compared with commercial rotary drill rigs and cable-suspended thermal core drills; and (3) auger drills are more environmentally friendly as they do not need to use a drilling fluid.

The main feature of electromechanical auger drills is that the rotating core barrel with helical flights on the outer surface is used to transport ice cuttings from the drill head to the imbedded chip chamber. The upper part of a typical drill includes (Fig. 1): (1) cable termination to connect the drill with the armored cable; (2) in most drills, a slip-ring device to prevent cable damage when the anti-torque fails, and a rotation sensor to detect anti-torque failure during penetration; (3) an anti-torque system to prevent spinning of the non-rotated section; (4) in some drills, a hammer to ease core breaking and retrieve a sticking drill; and (5) not always, a pressure-resistant instrumentation chamber, containing the sensors and controls.
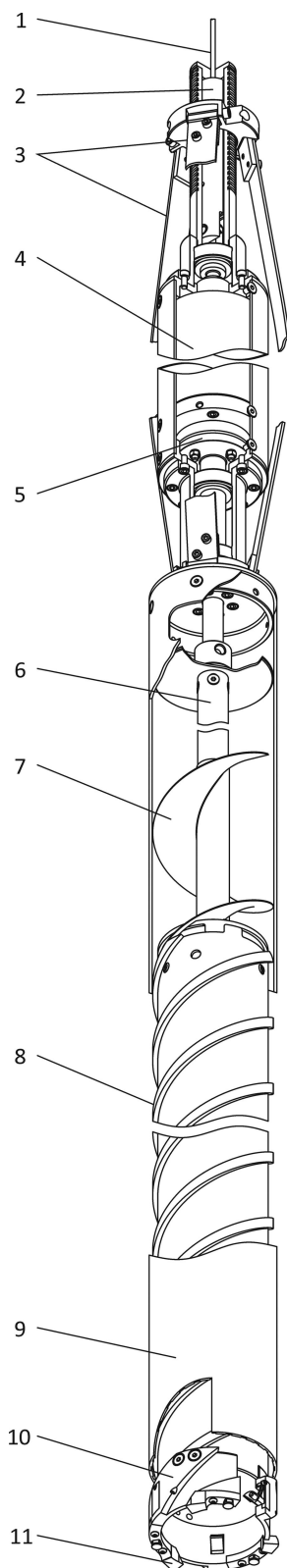
The lower part of the electromechanical auger drill includes: (1) a coring head equipped with cutters and core catchers; (2) a core barrel with spiral flights and chip chamber; (3) in most drills, a jacket; and (4) a geared motor. Torque limiters (friction clutch) were included in some drill designs. Some methods to increase friction between cuttings and the inner surface of the jacket (e.g. ribs or grooves) are provided in most of the drills.

The original concept of an electromechanical auger drill was based on the SIPRE hand auger driven by a suspended motor with an anti-torque device (Suzuki, 1994). Two such drills were built by Japanese experts in the early 1970s and tested at Mizuho station, Antarctica, in 1971 and at Ice Island T-3, Arctic Ocean, in 1973. At the same time, another auger drill was built at the University of Iceland, Reykjavík, and used in summer 1972 to drill a 415 m deep hole on Vatnajökull, Iceland (Árnason and others, 1974). Shortly afterwards, two other drills were designed at the University of Bern, Switzerland, by H. Rufli (Rufli and others, 1976) and at the US Army Cold Regions Research and Engineering Laboratory (CRREL) by J. Rand (Rand, 1976). The last two drills became for a long time excellent prototypes for electromechanical auger drills development, so this type of drill was often referred to as the 'Rufli–Rand drill'.

Dozens of electromechanical auger drills have been designed during the past few decades, yet one of the first holes on Vatnajökull is still recognized as the deepest hole drilled by this type of drill. The borehole at Vatnajökull was filled with drained water (Árnason and others, 1974). The details of the various internal components give each electromechanical auger drill its own unique operating capacities. However, the auger options were usually determined by experience, and the main parameters (auger angle and rotation speed) are varied in a wide range from drill to drill (Table 1).

Inability to promptly remove the cuttings results in their being pulverized into progressively finer particle sizes, making drilling very inefficient, and in extreme cases halting the drilling process altogether, resulting in cutters icing, abnormal power consumption and high rotation torques (Zacny and Cooper, 2007). This paper presents research on ice auger transportation based on the discrete element method (DEM)

Fig. 1. Basic structure of ice shallow drill: 1. cable; 2. cable termination; 3. anti-torque leaf springs; 4. motor with reducer; 5. clutch; 6. shaft; 7. booster; 8. rotating core barrel; 9. jacket; 10. drill head; 11. cutters.

which is able to analyze the performance of cuttings transportation depending on different operating conditions (auger angle and rotation speed) in terms of average particle velocity, average particle axial velocity, mass flow rate, average height of particle transportation, average particle unit mass, dissipated energy and energy distribution.

MODEL DESCRIPTION

The main elements of the auger conveyer are (Fig. 2):

D_1: auger inner diameter (ID) equal to the outer diameter (OD) of the core barrel;

D_2: auger OD or diameter of flights;

α: auger angle determined by the angle between the tangent to the flight helical line and a horizontal line;

p: pitch equal to the width of one complete helix turn measured parallel to the auger.

Auger angle is slightly changed from α_1 estimated on the auger ID to α_2 on the OD:

$$\alpha = \arctan \frac{p}{\pi D}, \qquad (1)$$

where D is the diameter (m) at an arbitrary point of the flight ($D_1 \leq D \leq D_2$).

Augers are often used for transporting, elevating or mixing particles at controlled and steady rates in agriculture or food processing (Owen and Cleary, 2009) and are employed in pile foundation engineering (Tan and others, 2011). Although the structures of augers differ, the principles applied in transporting cuttings or particles are always similar. Surprisingly, calculations based on the theory of auger transportation for soils suggested by Bashkatov and Olonovsky (1968) gave very small optimal auger angles (7.5–12°) for transportation of ice cuttings, contrary to field experience (Hong and others, 2014). This was a reason for undertaking this research and use of the DEM method to predict the performance of ice cuttings transportation by coring auger.

DEM simulations involve following the motion of every particle (coarser than some cut-off size) and modeling each collision between the particles and between the particles and their environment (e.g. the internal surface of the stationary jacket, the surface of the rotating core barrel and the surface of the flights). The boundary geometry is built using a CAD software package imported as a triangular surface mesh into the DEM software package. This provides unlimited flexibility in specifying the three-dimensional geometries with which the particles interact (Owen and Cleary, 2009).

The following considerations and parameters of the coring auger are applied to the simulation. The auger has three 5 mm wide flights at constant helix angle. The core barrel with an OD of 108 mm is modeled as a solid tube to keep cuttings in the gap between the core barrel and the jacket with ID/OD of 119/125 mm. The clearance between the auger flights and the inner surface of the jacket is 0.5 mm. A solid ring imitates the bottom of the hole to prevent falling-down of the cuttings from the flights due to gravitational force. A series of DEM simulations was carried out for different rotation speeds in the range 50–200 rpm and auger angles in the range 15–45° (Table 2). Since the processing time for each numerical experiment using a workstation based on an Intel Xeon E5-1650 processor was up to 4 months, the simulation time had to be limited to 0.4–1.0 s (the slower the rotation speed, the longer the simulation time).

The size analyses of the particles produced by the KEMS-112 electromechanical drill with air reverse circulation suggested that the 'cold' ice cuttings had an isometric shape that could be approximated by a ball (Talalay, 2006). In these DEM simulations, it is assumed that the maximum size
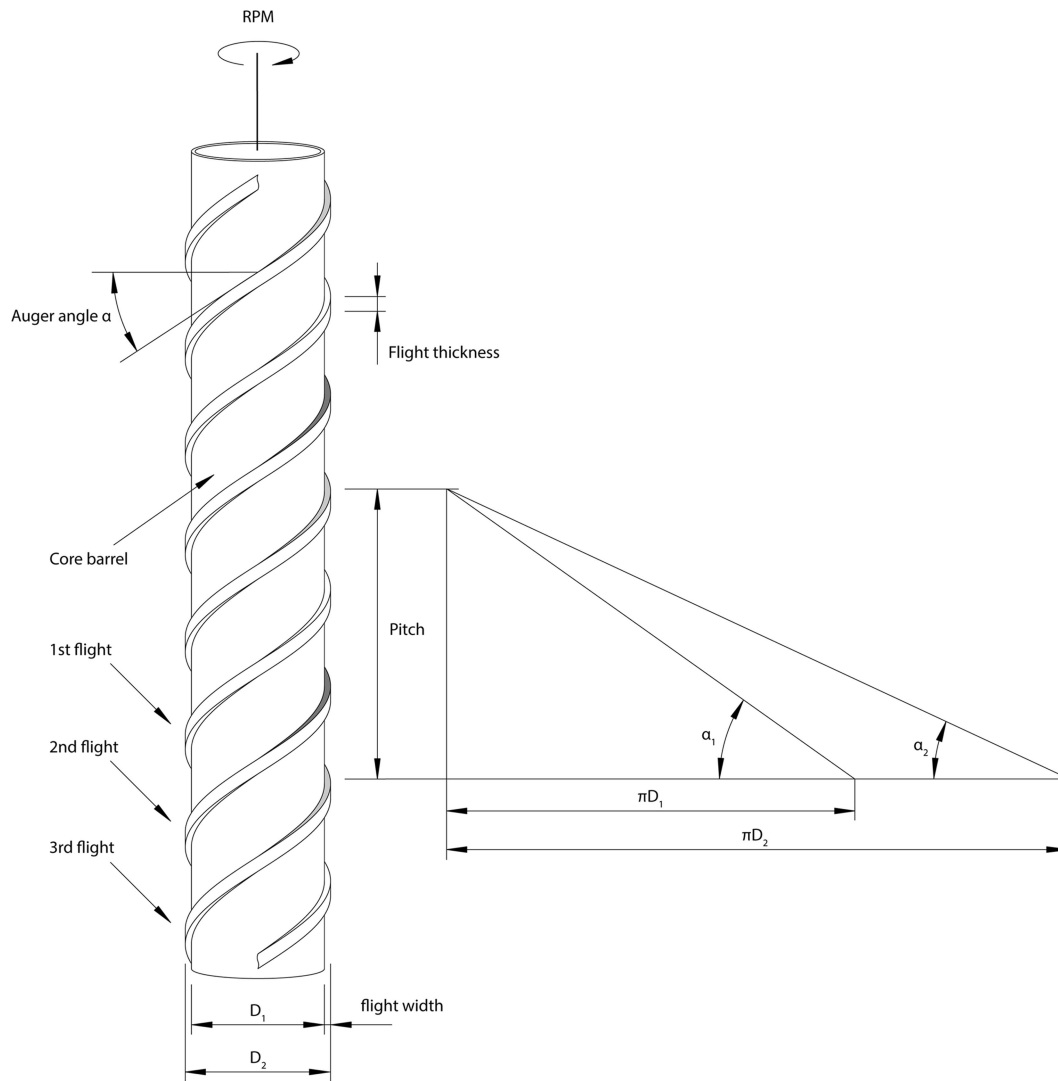
Fig. 2. Parameters of three-flight auger.

(diameter) of the ice particles is approximately equal to the depth of cut:

$$d \approx \frac{\text{ROP}}{60nm},\tag{2}$$

where ROP is the rate of penetration (in all simulations ROP = 20 m h^{-1}), n is the drill head rotation speed (rpm) and m is the number of cutters ($m = 3$). The particle sizes follow a normal distribution.

The mass of cuttings Q (kg s^{-1}) produced per unit time by the drill head is estimated as

$$Q = \frac{\pi\rho(d_2^2 - d_1^2)}{14.4 \times 10^3}\text{ROP},\tag{3}$$

where ρ is the density of drilled ice ($\rho = 920$ kg m^{-3}) and d_2 and d_1 are the OD/ID of the drill head ($d_2 = 0.129$ m; $d_1 = 0.1$ m).

The particle-to-particle (ice-to-ice) friction is taken as 0.1, that of particle to core-barrel (stainless steel) as 0.17, that of particle to flight (nylon) as 0.21 and that of particle to inner surface of the jacket (aluminum grooved tube) as 0.24.

CUTTINGS DISTRIBUTION ALONG THE AUGER

Figure 3 illustrates the cuttings distribution along the coring auger during transportation. The first row shows the particle distribution at a rotation speed of 50 rpm with the angle varied from 15° to 45° in steps of 10°. The rotation speed increases from 50 rpm to 200 rpm from the first row to the last (seventh) row in steps of 25 rpm. The cuttings are colored depending on their diameter, with the smaller particles being brighter and the larger particles darker.

At low rotation speeds (50 and 75 rpm) the particles are aligned with the auger flights at the slight angles of 15° and 25°. If the auger angle increases (35° and 45°), a cuttings build-up is formed near the bottom of the coring auger, indicating that the lifting force between cuttings and jacket is not enough to transport particles at these operating parameters.

At a rotation speed of 100 rpm, cuttings are transported smoothly without a build-up forming; however, at the highest auger angle of 45°, particles start to fall down in the clearance between the flights and the jacket. With a further increase in rotation speed, there is little evidence that cuttings form a build-up, but the number of cuttings that drop into the clearance between the flights and jacket increases. The particle sizes as shown by Eqn (2) decrease with increasing rotation speed and are smaller than the clearance between the flights and jacket (0.5 mm) at rotation speeds higher than 125 rpm. Downfallen particles need to be re-transported and can accumulate near the bottom,

Table 1. Main auger characteristics of shallow electromechanical drills

Institute or drill type	Inner/outer diameters			Flights pitch	Auger angle	Number of spirals	Rotation speed of auger	Source
	Drill head	Core barrel	Jacket					
	mm	mm	mm	mm	°		rpm	
University of Iceland, Reykjavík	90/120	91/95	106/110	200–260	35–42.3	2	150	Árnason and others (1974)
University of Bern, Switzerland	75/114.5	80/–	–/113	–	–	2	90	Rufli and others (1976)
CRREL, USA	100/142	100/108	132/140	200	32.5	2	100	Rand (1976)
UCPH, Denmark	78/104	81/85	97.6/101.6	180	35.3	3	75	Johnsen and others (1980)
National Hydrology Research Institute, Calgary, Canada	100/144	104.7/108	136.4/139.7	220	33.8	3	103	Holdsworth (1984)
PICO-4″, USA	102/142	–	–	–	–	2	60–200	Litwak and others (1984)
ILTS-130, Japan	107/140	110.1/114.3	131/135	200	30	2	100	Suzuki (1984)
AWI, Germany	75/117	81/–	106/110	–	–	3	175	Jessberger and others (1984)
LGGE, France	100/144	104/108	136/140	150	24.7	3	105	Gillet and others (1984)
Australian Antarctic Division, Kingston, Australia	93/131	–	–/128	–	–	3	35–130	Wehrle (1985)
BZXJ, China	67/91	72/74	–	194	39	3	50	Zhu and Han (1994)
ECLIPSE, Canada	82/–	–/89	–/108	178	34	3	50–75	Blake and others (1998)
BPRC, USA	100/129	–	–	–	–	–	–	Zagorodnov and others (2000)
FELICS, Switzerland	76/103	78/–	absence	–	–	2	220	Ginot and others (2002)

causing packing, increasing power consumption and finally a halt to cuttings transportation.

The results of cuttings distribution analysis show that there are two main types of particle transportation: an ordered track generated at lower rotation speeds, and a disordered track at rotation speeds higher than 125 rpm when cuttings are in a muddle along the auger. Comparing the rows in Figure 3, it is worth noting that the efficiency of cuttings transportation increases with increasing rotation speed. Comparing columns, it may be concluded that the efficiency of cuttings transportation increases with increasing auger angle.

RESULTS

The performance of cuttings transportation is studied in terms of the following parameters:

1. Average particle velocity (AV), which refers to the total velocity in three-dimensional space to describe how fast the cuttings move;

2. Average particle axial velocity (AAV), which refers to the velocity in the upward direction and relates to the vertical movement ability of the particles;

3. Mass flow rate (MFR), determined by recording the mass of each particle that has passed through a plane perpendicular to the axis of the screw (this plane is located halfway between the two periodic boundaries which are borders of a pitch; Owen and Cleary, 2009);

4. Average particle height (AH), which refers to the transportation height of particles to calculate the auger volumetric removal efficiency and to demonstrate its capability more clearly than velocity;

5. Average particles unit mass dissipated energy (AE), which refers to the energy consumed by 1 kg of particles being transported along the coring auger;

6. Energy ratio (ER), which indicates the ratio between particle kinetic energy and potential energy (if the kinetic energy of a particle is equal to its potential energy, ER = 1).

The AV marginally increases with increasing auger angle at low rotation speed (≤75 rpm) and increases more rapidly

Table 2. Selected and calculated auger operating parameters

Rotation speed	Auger angle	Particle size	Number of particles s^{-1}
rpm	°	mm	
50	15	1.11	5043
75	20	0.74	17 020
100	25	0.56	40 344
125	30	0.44	78 797
150	35	0.38	136 161
175	40	0.32	216 219
200	45	0.28	322 753

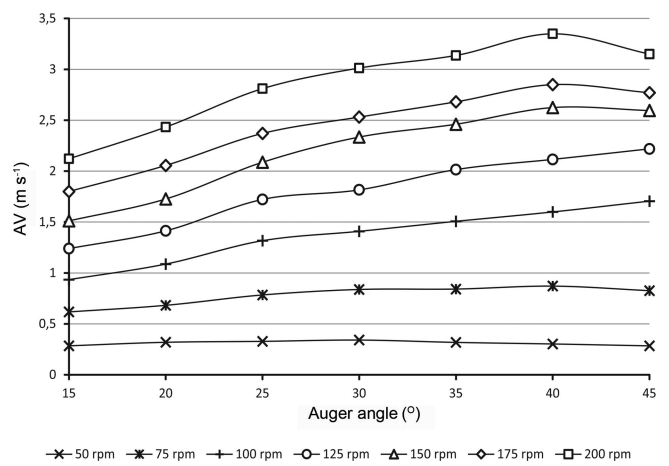**Fig. 3.** Cuttings distribution along coring auger.

Fig. 4. Average particle velocity (AV) vs auger angle.

The AAV trend is almost the same as AV (Fig. 5). The only difference is the curve shape at a rotation speed of 50 rpm in which AAV decreases more rapidly with increasing auger angle. This implies that, at low rotation speed, increasing the auger angle is an ineffective method to speed up the upward movement of the particles.

At first, the MFR rapidly increases with increasing auger angle and then starts to decelerate (Fig. 6). The turning point depends on the rotation speed: when the auger rotates at 50 and 75 rpm, MFR stabilizes at 30°; at 100 rpm at 35°; and at 125 and 150 rpm at 40°. The MFR at rotation speed >125 rpm and auger angle of 45° increases sharply, probably because disorder in the cuttings tracks causes some particles to pass the same plane many times. The MFR at a rotation speed of 50 rpm is lower than the others, which is in agreement with the slowest AAV.

The AH increases at the start and then becomes almost stable at certain auger angles depending on rotation speed: when the auger rotates at 50 rpm, AH stabilizes at 25°, and at 75 rpm at 35°, while at other rotation speeds AH starts to decelerate at 40° (Fig. 7). The variation of AH with auger angle is much smaller than the change due to increasing rotation speed, and the trend is almost the same as AAV.

The AE increases monotonically with increasing auger angle and rotation speed (Fig. 8). The variation of AE with auger angle is much smaller than the change due to
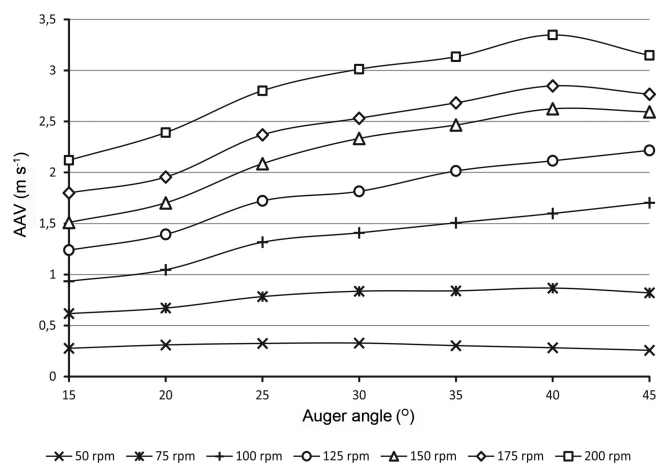
when the rotation speed exceeds 100 rpm (Fig. 4). At high rotation speed and steep helix angle (45°), the AV decreases. The variation of the AV with auger angle is smaller than the change due to the increase in rotation speed.

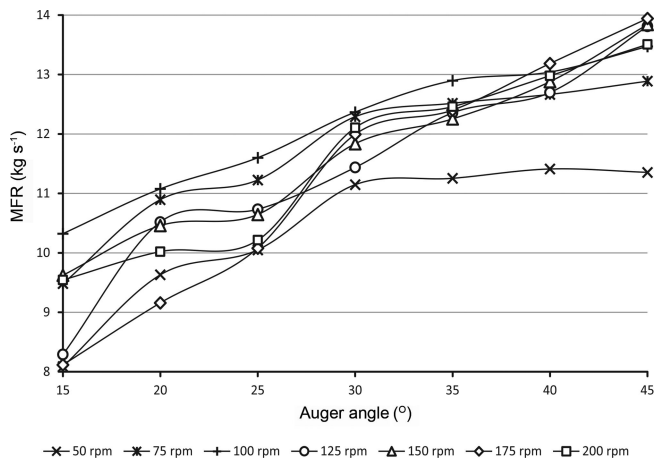**Fig. 5.** Average particle axial velocity (AAV) vs auger angle.

Fig. 6. Mass flow rate (MFR) of particles vs auger angle.
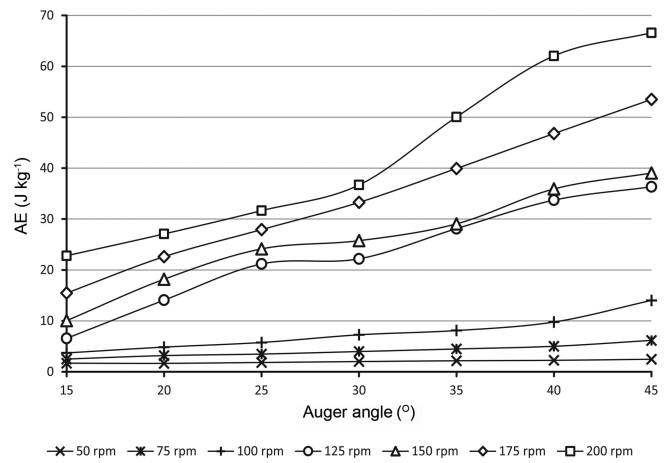

Fig. 8. Average particles unite dissipated energy (AE) vs auger angle.

increasing rotation speed. With rotation speed rising, the intensity of AE growth also rises, probably because of increased disordering of the cuttings tracks, which increases the kinetic energy of the particles.

The ER variations indicate that the portion of particle kinetic energy increases with increasing auger angle and rotation speed (Fig. 9). This is the main reason why AE increases with auger angle and rotation speed. The disordering of the particle tracks at large auger angle and high rotation speed consumes much more energy than regular transportation of cuttings.

CONCLUSIONS AND DISCUSSION

DEM simulation shows that the nature of cuttings transportation in a coring auger is complex and sensitive to the operating parameters. Considering the size of cuttings we can draw the following conclusions.

At low rotation speed, cuttings accumulate at the lower end of flights. At higher speed ($\geq$100 rpm), chip transportation is more efficient.

Assuming that particle size decreases with increase in rotation speed, more and more particles fall into the clearance between the flight and the jacket, with rotation speed increasing, resulting in a need for them to be transported over

again. Cuttings transportation is more efficient if the particle size is larger than the clearance between the flight and the jacket. Therefore generation of coarser cuttings should be considered when selecting the operating parameters (in the first instance, depth of cut and rotational speed) and shape of cutters. On the other hand, the clearance between the flight and the jacket has to be as small as possible. This depends on the coaxiality of the core barrel and jacket and the straightness of the tubes used to manufacture the core barrel and jacket, which is usually longer.

Maintaining an ordered track for the particles is an important factor in increasing transportation efficiency and energy saving. The reason why the cuttings tracks become disordered is probably that the clearance between the flights and jacket is larger than the diameter of the particles at high rotational speeds or that the weight of the particles is too light and the track easily becomes unstable at high rotation speed.

To choose optimal parameters for a coring auger, many factors have to be considered (e.g. particle sizes and their variability, ice temperature, material of core barrel and jacket and others, and the availability of the needed drive motor-gears). For the conditions assumed in the present study, the critical rotation speed between ordered tracking and disordered tracking is near 100 rpm at auger angles of
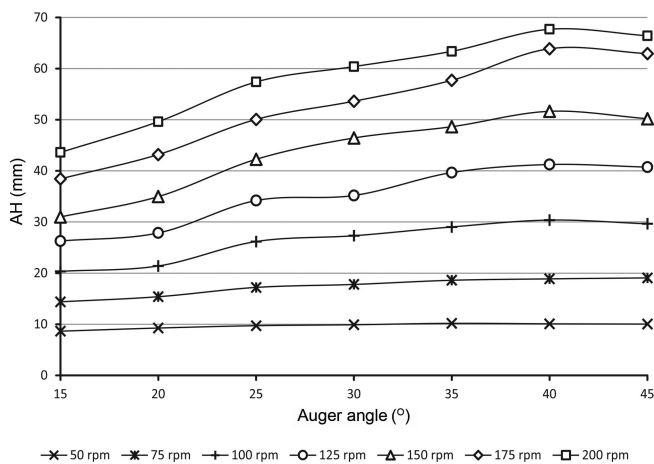

Fig. 7. Average height (AH) of particle transportation vs auger angle.
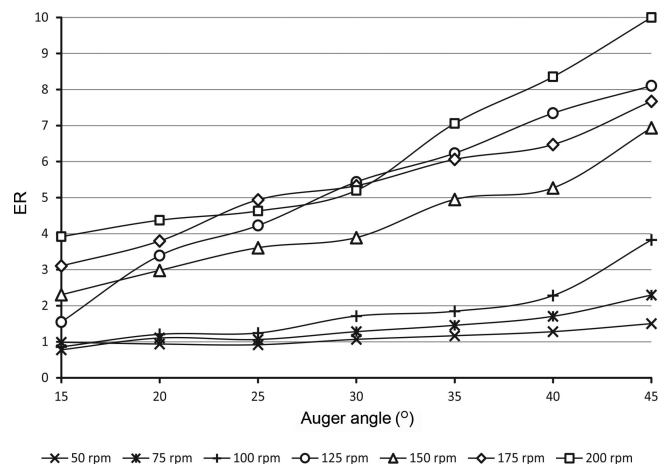

Fig. 9. Energy ratio (ER) of particles vs auger angle.

35–40°, and in conjunction with a comprehensive evaluation of various transportation characteristics (AV, AAV, AH, AE, ER) these values can be recommended as the optimal auger parameters.

ACKNOWLEDGEMENTS

REFERENCES

Árnason B, Björnsson H and Theodórsson P (1974) Mechanical drill for deep coring in temperate ice. *J. Glaciol.*, **13**(67), 133–139

Bashkatov DN and Olonovsky YA (1968) *Vrachshatel'noe shrekovoe bureniye geologorazvedochnikh skvazhin [Rotary auger prospecting drilling].* Nedra, Moscow

Blake EW, Wake CP and Gerasimoff MD (1998) The ECLIPSE drill: a field-portable intermediate-depth ice-coring drill. *J. Glaciol.*, **44**(146), 175–178

Gillet F, Donnou D, Girard C, Manouvrier A, Rado C and Ricou G (1984) Ice core quality in electro-mechanical drilling. *CRREL Spec. Rep.* 84-34, 73–80

Ginot P, Stampfli F, Stampfli D, Schwikowski M and Gäggeler HW (2002) FELICS, a new ice core drilling system for high-altitude glaciers. *Mem. Natl Inst. Polar Res.*, Special Issue 56, 38–48

Holdsworth G (1984) The Canadian Rufli–Rand electro-mechanical core drill and reaming device. *CRREL Spec. Rep.* 84-34, 21–32

Hong J, Talalay P and Sysoev M (2014) Optimization of ice cuttings transportation by cable-suspended core auger drills. *Global Geol.*, **17**(1), 48–54

Jessberger HL and Dörr R (1984) Recent experiences with a modified Rufli ice drill. *CRREL Spec. Rep.* 84-34, 45–49

Johnsen SJ, Dansgaard W, Gundestrup N, Hansen SB, Nielsen JO and Reeh N (1980) A fast light-weight core drill. *J. Glaciol.*, **25**(91), 169–174

Litwak J, Kersten L and Kuivinen K (1984) The PICO intermediate-drill system. *CRREL Spec. Rep.* 84-34, 41–44

Owen PJ and Cleary PW (2009) Prediction of screw conveyor performance using the Discrete Element Method (DEM). *Powder Technol.*, **193**(3), 274–288 (doi: 10.1016/j.powtec.2009.03.012)

Rand JH (1976) The USA CRREL shallow drill. In Splettstoesser JF ed. *Ice-core drilling*. University of Nebraska Press, Lincoln, NB, 133–137

Rufli H, Stauffer B and Oeschger H (1976) Lightweight 50-meter core drill for firn and ice. In Splettstoesser JF ed. *Ice-core drilling*. University of Nebraska Press, Lincoln, NE, 139–153

Suzuki Y (1984) Light weight electromechanical drills. *CRREL Spec. Rep.* 84-34, 33–40

Suzuki Y (1994) Development of Japanese mechanical drills – personal reminiscences. *Mem. Natl Inst. Polar Res.*, Special Issue 49, 1–4

Talalay PG (2006) Removal of cuttings in deep ice electromechanical drills. *Cold Reg. Sci. Technol.*, **44**(2), 87–98 (doi: 10.1016/j.coldregions.2004.08.005)

Tan SC, Duan LC, Tan SE and Shi H (2011) Study on critical drilling parameters for auger drilling. *Adv. Mater. Res.*, **243–249**, 3331–3340 (doi: 10.4028/www.scientific.net/AMR.243-249.3331)

Wehrle E (1985) A shallow core-collecting mechanical ice drill. *ANARE Res. Notes,* **28**, 196–201

Zacny KA and Cooper GA (2007) Methods for cuttings removal from holes drilled on Mars. *Mars*, **3**, 42–56 (doi: 10.1555/mars.2007.0004)

Zagorodnov V, Thompson LG and Mosley-Thompson E (2000) Portable system for intermediate-depth ice-core drilling. *J. Glaciol.*, **46**(152), 167–172 (doi: 10.3189/172756500781833304)

Zhu G and Han J (1994) BZXJ super light ice core drill. *Mem. Natl Inst. Polar Res.*, Special Issue 49, 87–92